Journal of Chemical Neuroanatomy 104 (2020) 101745

Contents lists available at ScienceDirect

Journal of Chemical Neuroanatomy

journal homepage: www.elsevier.com/locate/jchemneu

Calbindin immunostaining in the CA1 hippocampal pyramidal cell layer of the human and mouse: A comparative study

Paula Merino-Serrais[a,b,1], Silvia Tapia-González[a,b,c,1], Javier DeFelipe[a,b,c,*]

[a] Departamento de Neurobiología Funcional y de Sistemas, Instituto Cajal, CSIC, Madrid, Spain
[b] Laboratorio Cajal de Circuitos Corticales (CTB), Universidad Politécnica de Madrid, Madrid, Spain
[c] Centro de Investigación Biomédica en Red sobre Enfermedades Neurodegenerativas (CIBERNED), ISCIII, Madrid, Spain

ARTICLE INFO

Keywords:
Calcium binding proteins
Pyramidal neuron
Non-pyramidal neuron
Postmortem time delay
Species differences

ABSTRACT

Immunostaining for calbindin (CB) is commonly used to label particular populations of neurons. Recently, it has been shown that the CA1 pyramidal cells in the mouse can be subdivided along the radial axis into superficial and deep pyramidal cells and that this segregation in the radial axis may represent a general principle of structural and functional organization of the hippocampus. One of the most widely used markers of the superficial pyramidal cells is CB. However, this laminar segregation of pyramidal cells has not been reported in the human CA1 using CB immunostaining. The problem is that the different pattern of CB immunostaining observed in the mouse compared to the human could be explained by technical features, of which one of the most important is the postmortem time (PT) delay typical of the brain tissue obtained from humans. In the present study, we have studied the influences of PT delays and fixation procedures and we found that the clear differences found between the CA1 of the human and mouse do not depend on the fixation, but represent actual species-specific differences. These remarkable differences between species should be taken into consideration when making interpretations in translational studies from mouse to human brains.

1. Introduction

Many neurons of the vertebrate central nervous system express the calcium binding protein calbindin D-28k (CB). CB immunostaining has been used as a marker for different brain regions and to distinguish separate populations of neurons, including pyramidal and non-pyramidal cells (e.g., Celio, 1990; DeFelipe, 1997). Recently, it has been shown that —rather than being a homogenous population of cells— CA1 pyramidal cells in the mouse can be subdivided along the radial axis into superficial and deep pyramidal cells, which differ in terms of a number of characteristics regarding genetics, morphology, connectivity, and electrophysiology (Danielson et al., 2016; Fattahi et al., 2018; Geiller et al., 2017; Soltesz and Losonczy, 2018). It has been proposed that this segregation based on the radial axis may represent a general principle of organization in the hippocampus that increases the capacity of the hippocampus to compute and process several tasks in parallel (Fattahi et al., 2018; Geiller et al., 2017). One of the most commonly used markers of the superficial pyramidal cells in the mouse is CB. However, the laminar segregation of pyramidal cells described above has not been reported in the human CA1 using immunostaining for CB (Ding and Van Hoesen, 2015; Seress et al., 1992, 1993; Sloviter et al., 1991; Arellano et al., 2004). Nevertheless, the description of the pattern of immunostaining in the human CA1 differs between different laboratories. For example, Sloviter et al. (1991) and Ding and Van Hoesen (2015) did not observe CB-immunoreactive (-ir) pyramidal cells in CA1 (most were non-pyramidal cells), whereas Seress et al. (1992, 1993), Wittner et al. (2002), Abrahám et al. (2009), and Maglóczky (2010) reported relatively high numbers of labeled pyramidal cells. The divergent observations from human hippocampal CA1 and the different pattern of CB immunostaining observed in the mouse compared to the human could be explained by technical features. For example, using different fixatives or differences in the fixation procedure —brain tissue obtained after perfusion versus immersion-fixed brain tissue extracted immediately after death (postmortem time [PT] 0 h, 0 min) or after several PT delays— have been shown to alter a number of metabolic and immunostaining characteristics of the brain tissue (e.g., Gonzalez-Riano et al., 2017; Lavenex et al., 2009). However, it is common to describe similar or different patterns of immunostaining when comparing brain tissue from humans with experimental animals without considering these critical methodological factors. Therefore, it is not

* Corresponding author at: Instituto Cajal, Departamento de Neurobiología Funcional y de Sistemas, Avenida Doctor Arce 37, Madrid, 28002, Spain.
E-mail address: defelipe@cajal.csic.es (J. DeFelipe).
[1] These authors contributed equally to this work.

https://doi.org/10.1016/j.jchemneu.2020.101745
Received 28 November 2019; Received in revised form 4 January 2020; Accepted 10 January 2020
Available online 13 January 2020

Table 1
Summary of technical information of the human cases. The human case codes are internal codes to ensure the confidentiality of each human sample.

Human case code	Age (y)	Sex	Postmortem delay (h:min)	Source	Fixation procedure
M8	69	Male	2:30	Autopsy	Immersion-fixed
M7	49	Male	2	Autopsy	Immersion-fixed
AB3	53	Male	3:20	Autopsy	Immersion-fixed
AB2	50	Female	4	Autopsy	Immersion-fixed
H65	21	Female	–	Biopsy*	Immersion-fixed

*Non sclerotic hippocampus obtained from postoperative tissue samples (biopsy) from an epileptic patient suffering from pharmacoresistant temporal lobe epilepsy. See Materials and Methods for further information.

clear to what extent technical factors account for the different observations between human and mouse CA1 —as well as the differences found by different laboratories— and to what extent such differences can be attributed to actual species-specific differences.

In the present study, we have further examined possible influences of PT delays, fixation procedures, and different fixative solutions on the patterns of CB immunostaining in both human and mouse CA1.

2. Material and methods

2.1. Human brain tissue

Two types of human hippocampal samples were used in the present study: autopsy samples —from 4 control cases (PT between 2 and 4 h)— and biopsy samples from postoperative tissue samples from an epileptic patient suffering from pharmacoresistant temporal lobe epilepsy (TLE) with a hippocampus without histopathological alterations (Table 1). This tissue has been used in previous studies where detailed information about the cases can be found (Arellano et al., 2004; Arion et al., 2006; Kastanauskaite et al., 2009; Inda et al., 2007; Muñoz et al., 2007; Tapia-González et al., 2019). The tissue was obtained following national laws and international ethical and technical guidelines on the use of human samples for biomedical research purposes.

Upon removal, the human brains were immediately fixed in cold 4% paraformaldehyde (PFA) in phosphate buffer (0.1 M, pH 7.4) and small blocks of the hippocampal formation and adjacent cortex were then obtained and post-fixed in the same fixative solution for 24 h at 4 °C. After fixation, vibratome sections of the cortical tissue (50 μm) were obtained and processed for histology or immunostaining.

2.2. Mouse brain tissue

In order to perform comparative studies between humans and mice in the present study, we examined CB-ir in two groups of mice as described in our previous study (Gonzalez-Riano et al., 2017). Two-month-old male C57BL/6 J mice (Charles River Laboratories, Wilmington, MA) were used in both groups. Animals were kept in a 12:12-h light/dark cycle and received food and water ad libitum. All experimental protocols involving the use of animals were performed in accordance with recommendations for the proper care and use of laboratory animals, and under the authorization of the regulations and policies governing the care and use of laboratory animals [EU directive no. 86/609 and Council of Europe Convention ETS1 23, EU decree 2001-486 and Statement of Compliance with Standards for Use of Laboratory Animals by Foreign Institutions no. A5388-01, National Institutes of Health (USA)]. Special care was taken to minimize animal suffering and to reduce the number of animals used to the minimum required for this study.

The animals from the first group (n = 3) were anaesthetized with a lethal pentobarbital injection (40 mg/kg BW, Vetoquinol, Madrid, Spain) and transcardially perfused with a saline solution followed by 4% PFA in PB. The brains were removed, post-fixed by immersion in the same fixative for 20 h at 4 °C and cryoprotected in 30% sucrose. To test the possible effects of PT on CB immunostaining, we used a second group of mice that were sacrificed with the same pentobarbital lethal injection as described above. Thereafter, their brains were removed at 0, 2 and 5 h PT, respectively (n = 3 mice, per interval), fixed in 4% PFA in PB overnight (20 h) at 4 °C. Thereafter, the brains from the two groups of animals were cut into 50-μm-thick coronal slices with a freezing sliding microtome (Microm HM 450, Microm International, Germany) and processed for immunocytochemistry (immunoperoxidase and immunofluorescence).

2.3. Immunohistochemistry

Single immunohistochemistry was performed in free-floating human and mouse sections. The sections were first pre-treated with 2% H_2O_2 for 30 min to remove the endogenous peroxidase activity and the slices were then blocked for 1 h in PB (0.1 M) with 0.25% Triton X-100 and 3% normal goat serum (Vector Laboratories Inc., Burlingame, CA, USA). Then, the sections were incubated overnight at 4 °C with the primary antibody rabbit anti-calbindin D28 K (CB-38a; Swant, Switzerland; 1:2000). On the following day, the sections were rinsed in PB and incubated for 2 h with biotinylated goat anti-rabbit IgG antibody (BA2000, Vector laboratories, Burlingame, CA; 1:250). After several washes in PB, the sections were incubated for 1 h at room temperature with avidin–biotin peroxidase complex (Vectastain ABC Elite PK6100, Vector; diluted 1:125). The staining was then performed with 0.01% hydrogen peroxide with 3, 3´ diaminobenzidine tetrahydrochloride chromogen (DAB: Sigma-Aldrich, St. Louis, MO, USA). All sections were incubated until they turned light brown, with the same duration of incubation for all slides; the immunostaining was checked via light microscope before stopping the reaction in all slides. Then, the sections were incubated in 0.02% OsO_4 in PB for 15 s at room temperature. Finally, the sections were mounted, dehydrated and cleared with xylene and coverslipped with DPX (Fluka AG, Buchs, Switzerland). Sections from every patient were Nissl-stained in order to identify the cortical areas and the laminar boundaries.

For immunofluorescence, free-floating sections were blocked for 1 h in PB with 0.25% Triton X-100 and 3% normal goat serum and incubated overnight at 4 °C with the antibody rabbit anti-calbindin D28 K (CB-38a; Swant, Switzerland; 1:2000). The sections were then rinsed in PB and incubated for 2 h at room temperature with Alexa Fluor 594-conjugated goat anti-rabbit antibody (A11012, Molecular Probes, Madrid, Spain; 1:1000). The nuclei from every mouse section were counterstained with DAPI (4, 6-diamidino-2-phenylindole) (Sigma, San Louis; MO; 1:80). To eliminate lipofuscin autofluorescence in human samples, eliminator reagent (2160, Millipore) was used following the manufacturer's instructions. Finally, sections were mounted and coverslipped with ProLong ® Gold antifade reagent (Life technologies, Carlsbad, CA). To confirm the specificity of CB-38a for DAB and fluorescence immunostaining, negative controls were performed in parallel with the primary experiments, omitting the primary antibody under the same conditions.

To test the possible effects of different fixative solutions on CB immunostaining, prior to the above-mentioned immunostaining procedure, we exposed human and mouse brain sections already fixed with PFA to a mixture of 4% PFA and glutaraldehyde (0.125%) in PB for 1 h.

Fig. 1. CB-ir neurons show no sub-laminar distribution in human CA1 pyramidal cell layer. (A) Low-power photomicrograph of a section immunostained for CB from the hippocampal formation obtained from autopsy. (B) Higher magnification of the area indicated by a rectangle in A to show the pattern of immunostaining in CA1. (C) Representative image of CA2 taken from A. Arrows in C indicate some pyramidal neurons which are relatively numerous compared to CA1 (B). Or, stratum oriens; Pyr, stratum pyramidale; Rad, stratum radiatum; Alv, alveus; Scale bar shown in A indicates 1000 μm in A, 170 μm in B, and 120 μm in C.

3. Results

We performed immunostaining techniques which aimed to analyze possible effects of PT delay, fixation procedures and different fixative solutions on the pattern of CB-immunostaining in CA1 pyramidal cell layer from human and mouse brains. As previously discussed in Gonzalez-Riano et al. (2017), since small changes are typically found from experiment to experiment, subtle changes are difficult to interpret. Thus, we were only looking for large, obvious changes. Therefore, we qualitatively analyzed the staining pattern for CB in CA1 pyramidal cell layer of (i) the human hippocampal body according to the indications of the atlas of Mai et al. (2016) and (ii) the dorsal mouse hippocampus from Bregma −1.46 to −2.30 (Paxinos and Franklin, 2001).

3.1. CA1 pyramidal cell layer has a different distribution of CB-ir neurons in human compared with mouse

As shown in Fig. 1, CB-ir neurons in the human CA1 were distributed in the CA1 pyramidal cell layer without any apparent preference in the radial aspect. The vast majority of well-labeled neurons were identified as non-pyramidal cells by morphological criteria. In addition, some CB-ir neurons were identified as pyramidal neurons but they were rather scarce (Figs. 1B, 2 B, C, and 3 C, D). However, relatively numerous CB-ir pyramidal neurons were found in CA2 (Fig. 1C) in the same preparations. In the mouse CA1, CB-ir neurons were located mainly in the CA1 superficial layer (Fig. 4) forming a well stratified "CB-ir pyramidal cell layer". The relative proportions of the two types of CB-ir neuron were observed to be the opposite to that seen in humans: most CB-ir neurons were identified as pyramidal cells, whereas relatively few were identified as non-pyramidal neurons.

3.2. The pattern of CB distribution is not affected by different short PT delays or different fixative procedures

No changes in the general pattern of distribution of CB immunostaining throughout the CA1 pyramidal cell layer were observed in either human or mouse brains with PT up to 5 h (Figs. 1–4). However, we observed a slightly higher intensity in the immunostaining of the CA1 neuropil of the mouse brain fixed by immersion that was extracted immediately after death (PT, 0 h 0 min) (Fig. 4E and I) compared to perfused-fixed brain (Fig. 4D and H). Furthermore, we observed a lower immunostaining intensity in cell bodies, neuronal

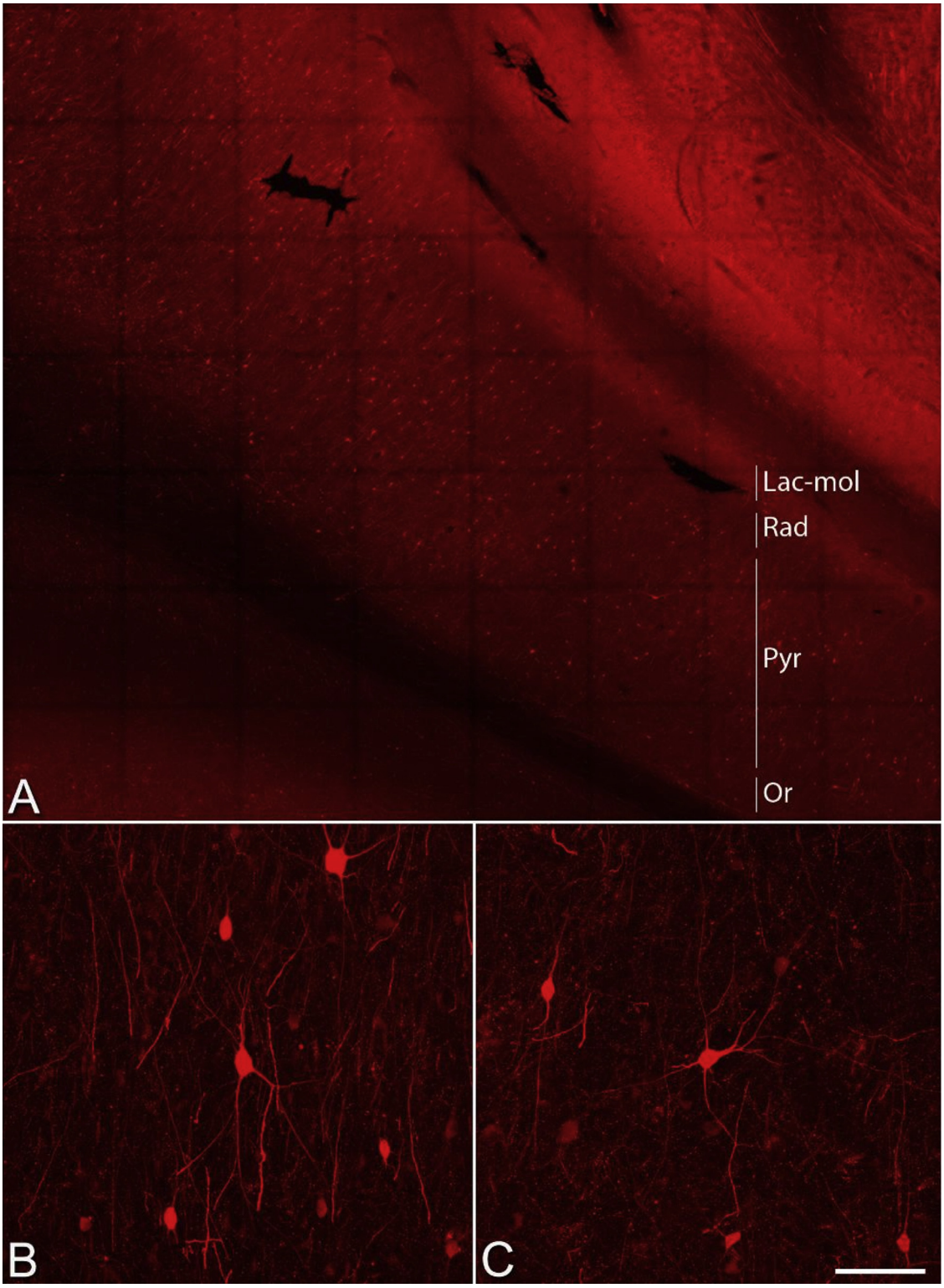

Fig. 2. Visualization of fluorescence-immunostained CB-ir neurons in sections from the human hippocampus. (A) CB fluorescence immunostained image showing a panoramic view of the hippocampus obtained from autopsy. Note that there is not a sub-laminar distribution of labeled neurons in the CA1 pyramidal cell layer. (B, C) Images taken from A at a higher magnification. The immunostaining is similar to that found in sections stained for DAB (see Fig. 1 B). Lac-mol, stratum lacunosum-moleculare; Or, stratum oriens; Pyr, stratum pyramidale; Rad, stratum radiatum; Alv, alveus. Scale bar shown in C indicates 800 μm in A, 50 μm in B and 50 μm in C.

processes and neuropil in immersion-fixed mouse tissue extracted after 2 h up to 5 h PT (Fig. 4F and J), as compared to tissue from perfused animals (Fig. 4D and H) or immersion-fixed mouse brain 0 h 0 min PT (Fig. 4E and I). Finally, we tested the possible effects on CB immunostaining in brain tissue fixed with a mixture of glutaraldehyde and paraformaldehyde. We found that the pattern of immunostaining did not change in either humans or mice (Figs. 3 and 4). Nevertheless, the inclusion of glutaraldehyde in the fixative produced a general

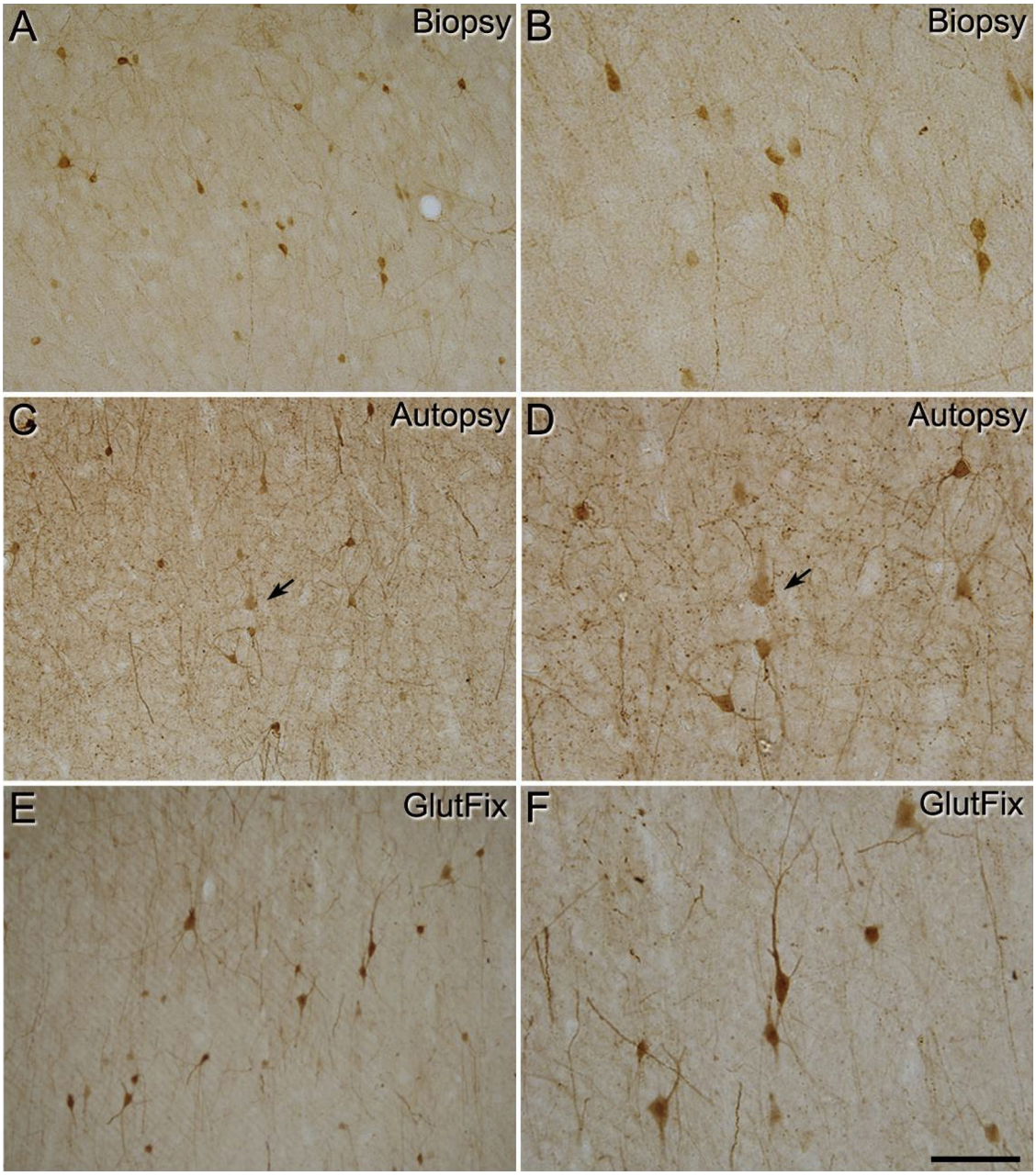

Fig. 3. Photomicrographs of sections immunostained for CB in the human CA1 pyramidal cell layer from case H65 (A) and case AB3 (C and E). B, D and F are higher magnifications of A, C and E, respectively. Arrows in C and D indicate a labeled pyramidal neuron. Sections shown in A and D were from brain tissue fixed in PFA, whereas the section shown in E, F was fixed with a mixture of PFA and glutaraldehyde. Scale bar shown in F indicates 70 µm in A, C, E, and 50 µm in B, D, F.

reduction in the background of the immunostaining in both human and mouse samples (Figs. 3E, F and 4 E, G).

4. Discussion and conclusion

In the present study, we further emphasize that there are clear differences in the pattern of immunostaining for CB in the CA1 of the human compared to the mouse, and that these differences do not depend on the fixation of the brain tissue but rather reflect actual species-specific differences.

The most remarkable differences are the following: most studies report that in the human, relatively few labeled neurons are present in CA1, where they are distributed without an obvious laminar preference, e.g., Sloviter et al. (1991); Ding and Van Hoesen (2015) and our own studies (although it should be noted that not all studies reached this conclusion; see Seress et al. (1992, 1993), Wittner et al. (2002), Abrahám et al., (2009), and Maglóczky (2010). Furthermore, both pyramidal and non-pyramidal neurons are labeled but the majority of well-labeled neurons can be identified as non-pyramidal cells. In the mouse, again both pyramidal cells and non-pyramidal cells are labeled but the labeled pyramidal cells are so numerous in the superficial aspect of the CA1 pyramidal cell layer that the labeled cells form a continuous row such that the superficial pyramidal cell layer of CA1 is clearly delimitated.

It is important to point out that the relatively few CB-ir cells present in the human CA1 observed in the present study is in line with the human transcriptome map obtained using *in situ* hybridization by Hawrylycz et al. (2012), showing that CB is strongly expressed in CA1 of the mouse but not in the human CA1. Furthermore, we found that CB-ir pyramidal cells are very numerous in the human CA2, which is

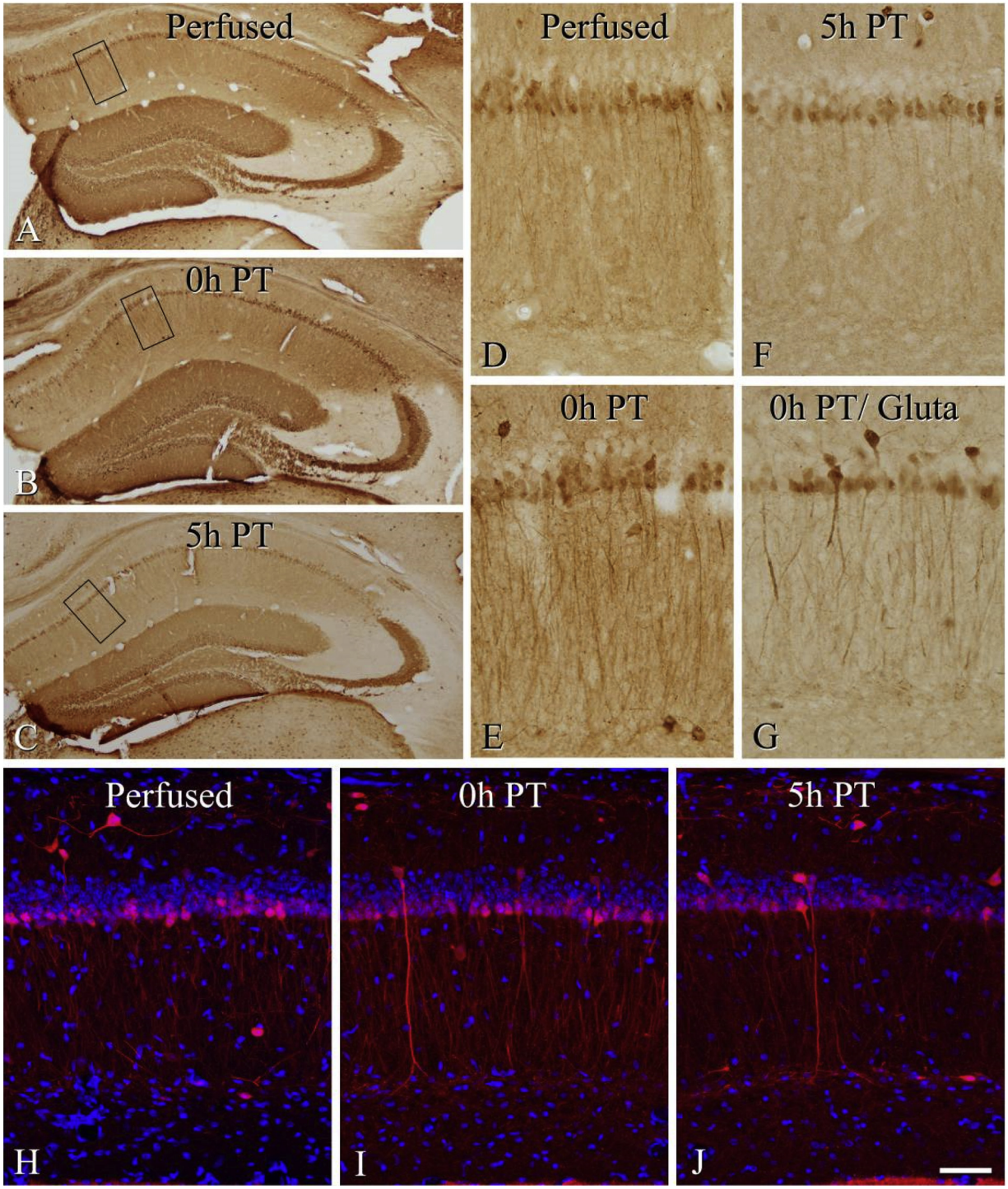

Fig. 4. CB-ir neurons show sub-laminar distribution in mouse CA1 pyramidal cell layer. CB immunostaining in mouse hippocampus under different experimental conditions. (A–C) Low-magnification photomicrographs showing CB immunostaining of sections from the hippocampus of a perfused brain (A), or fixed by immersion immediately after death (PT 0 h, 0 min) (B), or by immersion after 5 h PT (C). (D–G) High-magnification photomicrographs to show in greater detail the differences in immunostaining under different experimental conditions. The areas indicated by a rectangle in A, B and C are shown at a higher magnification in D, F and E, respectively. (H–J) Confocal images taken from the pyramidal cell layer of CA1 in sections immunostained for CB and counterstained with DAPI from a perfused mouse brain (H), or fixed by immersion immediately after death (PT 0 h, 0 min) (I), or by immersion after 5 h PT (J). Scale bar shown in J indicates 250 μm in A–C, 43 μm in D–G and 48 μm in H–J.

also consistent with the robust expression of CB observed using *in situ* hybridization. The present results further highlight species differences of the hippocampus with regard to a number of anatomical, neurochemical, genetic and physiological characteristics (e.g., Hof et al., 1996; Hawrylycz et al., 2012; Mashiko et al., 2012; Slomianka et al., 2013; Ding, 2013; van Dijk et al., 2016; Tapia-González et al., 2019; Benavides-Piccione et al., 2019). However, most studies emphasize the similarities between species, with the differences often not being considered when extrapolating data from the hippocampus from one species to another. For example, the obvious differences in the cytoarchitecture of CA1 between the human and mouse is often not taken into consideration when dealing with the functional and connectivity

interpretation of data obtained in mice and humans. As recently discussed in Benavides-Piccione et al. (2019), the consequences of the fact that the human pyramidal cell layer of CA1 is much less densely packed than that of the mouse is frequently ignored. This is sometimes referred to as "corticalization" of the human CA1 pyramidal cell layer because it resembles a neocortical cytoarchitecture. From the point of view of connectivity, this corticalization has an important impact on the local circuits since the basal and apical dendrites of human pyramidal cells are intermixed in the pyramidal cell layer, whereas —in the mouse— the basal and apical dendritic domains are basically separated (basal dendrites in the stratum oriens; apical dendrites in the stratum radiatum). In addition, to the differences in the expression of CB in the human and mouse pyramidal cells, human CA1 pyramidal cells are larger and have a different structural organization compared to mouse CA1 pyramidal cells regarding particular morphological features, which must reflect differences in cortical processing of information (Benavides-Piccione et al., 2019). In conclusion, the remarkable differences between species should be taken into consideration in order to make appropriate interpretations in translational studies from mouse to human brains.

Ethical Statement

The tissue was obtained following national laws and international ethical and technical guidelines on the use of human and experimental animal samples for biomedical research purposes.

CRediT authorship contribution statement

Paula Merino-Serrais: Investigation, Methodology. **Silvia Tapia-González:** Investigation, Methodology. **Javier DeFelipe:** Conceptualization, Methodology, Supervision.

Declaration of Competing Interest

The authors declare that the research was conducted in the absence of any commercial or financial relationships that could be construed as a potential conflict of interest.

Acknowledgements

We would like to thank Carmen Alvarez, Miriam Marín, and Lorena Valdes for their helpful technical assistance and Nick Guthrie for his excellent input regarding text editing. This work was supported by grants from the following entities: the Spanish Ministerio de Ciencia, Innovación y Universidades (Grants PGC2018-094307-B-I00 to JD and IJCI-2016-27658 to PMS); Centro de Investigación Biomédica en Red sobre Enfermedades Neurodegenerativas (CIBERNED, CB06/05/0066, Spain) and; the European Union's Horizon 2020 Research and Innovation Programme under grant agreement No. 785907 (HBP SGA2) (Human Brain Project).

References

Abrahám, H., Veszprémi, B., Kravják, A., Kovács, K., Gömöri, E., Seress, L., 2009. Ontogeny of calbindin immunoreactivity in the human hippocampal formation with a special emphasis on granule cells of the dentate gyrus. Int. J. Dev. Neurosci. 27, 115–127. https://doi.org/10.1016/j.ijdevneu.2008.12.004.

Arellano, J.I., Muñoz, A., Ballesteros-Yáñez, I., Sola, R.G., DeFelipe, J., 2004. Histopathology and reorganization of chandelier cells in the human epileptic sclerotic hippocampus. Brain 127 (Pt 1), 45–64. https://doi.org/10.1093/brain/awh004awh004. [pii].

Arion, D., Sabatini, M., Unger, T., Pastor, J., Alonso-Nanclares, L., Ballesteros-Yáñez, I., García Sola, R., Muñoz, A., Mirnics, K., DeFelipe, J., 2006. Correlation of transcriptome profile with electrical activity in temporal lobe epilepsy. Neurobiol. Dis. 22, 374–387. https://doi.org/10.1016/j.nbd.2005.12.012.

Benavides-Piccione, R., Regalado-Reyes, M., Fernaud-Espinosa, I., Kastanauskaite, A., Tapia-González, S., León-Espinosa, G., et al., 2019. Differential structure of hippocampal CA1 pyramidal neurons in the human and mouse. Cereb. Cortex. https://doi.org/10.1093/cercor/bhz122. pii: bhz122.

Celio, M.R., 1990. Calbindin D-28k and parvalbumin in the rat nervous system. Neuroscience 35 (2), 375–475.

Danielson, N.B., Zaremba, J.D., Kaifosh, P., Bowler, J., Ladow, M., Losonczy, A., 2016. Sublayer-specific coding dynamics during spatial navigation and learning in hippocampal area CA1. Neuron 91 (3), 652–665. https://doi.org/10.1016/j.neuron.2016.06.020. doi:S0896-6273(16)30298-7 [pii].

DeFelipe, J., 1997. Types of neurons, synaptic connections and chemical characteristics of cells immunoreactive for calbindin-D28K, parvalbumin and calretinin in the neocortex. J. Chem. Neuroanat. 14 (1), 1–19 doi:S0891061897100138 [pii].

Ding, S.-L., 2013. Comparative anatomy of the prosubiculum, subiculum, presubiculum, postsubiculum, and parasubiculum in human, monkey, and rodent. J. Comp. Neurol. 521, 4145–4162. https://doi.org/10.1002/cne.23416.

Ding, S.-L., Van Hoesen, G.W., 2015. Organization and detailed parcellation of human hippocampal head and body regions based on a combined analysis of cyto- and chemoarchitecture. J. Comp. Neurol. 523 (15), 2233–2253. https://doi.org/10.1002/cne.23786.

Fattahi, M., Sharif, F., Geiller, T., Royer, S., 2018. Differential representation of landmark and self-motion information along the CA1 radial Axis: self-Motion generated place fields shift toward landmarks during septal inactivation. J. Neurosci. 38 (30), 6766–6778. https://doi.org/10.1523/JNEUROSCI.3211-17.2018. doi:JNEUROSCI.3211-17.2018 [pii].

Geiller, T., Royer, S., Choi, J.S., 2017. Segregated cell populations enable distinct parallel encoding within the radial Axis of the CA1 pyramidal layer. Exp. Neurobiol. 26 (1), 1–10. https://doi.org/10.5607/en.2017.26.1.1.

Gonzalez-Riano, C., Tapia-Gonzalez, S., Garcia, A., Munoz, A., DeFelipe, J., Barbas, C., 2017. Metabolomics and neuroanatomical evaluation of post-mortem changes in the hippocampus. Brain Struct. Funct. 222 (6), 2831–2853. https://doi.org/10.1007/s00429-017-1375-510.1007/s00429-017-1375-5. [pii].

Hawrylycz, M.J., Lein, E.S., Guillozet-Bongaarts, A.L., Shen, E.H., Ng, L., Miller, J.A., et al., 2012. An anatomically comprehensive atlas of the adult human brain transcriptome. Nature 489, 391–399. https://doi.org/10.1038/nature11405.

Hof, P.R., Rosenthal, R.E., Fiskum, G., 1996. Distribution of neurofilament protein and calcium-binding proteins parvalbumin, calbindin, and calretinin in the canine hippocampus. J. Chem. Neuroanat. 11, 1–12.

Inda, M.C., DeFelipe, J., Munoz, A., 2007. The distribution of chandelier cell axon terminals that express the GABA plasma membrane transporter GAT-1 in the human neocortex. Cereb. Cortex 17 (9), 2060–2071. https://doi.org/10.1093/cercor/bhl114. doi:bhl114 [pii].

Kastanauskaite, A., Alonso-Nanclares, L., Blazquez-Llorca, L., Pastor, J., Sola, R.G., DeFelipe, J., 2009. Alterations of the microvascular network in sclerotic hippocampi from patients with epilepsy. J. Neuropathol. Exp. Neurol. 68 (8), 939–950.

Lavenex, P., Lavenex, P.B., Bennett, J.L., Amaral, D.G., 2009. Postmortem changes in the neuroanatomical characteristics of the primate brain: hippocampal formation. J. Comp. Neurol. 512 (1), 27–51. https://doi.org/10.1002/cne.21906.

Maglóczky, Z., 2010. Sprouting in human temporal lobe epilepsy: excitatory pathways and axons of interneurons. Epilepsy Res. 89 (1), 52–59. https://doi.org/10.1016/j.eplepsyres.2010.01.002.

Mai, J., Majtanik, M., Paxinos, G., 2016. Atlas of the Human Brain, 4th ed. Academic Press, San Diego.

Mashiko, H., Yoshida, A.C., Kikuchi, S.S., Niimi, K., Takahashi, E., Aruga, J., et al., 2012. Comparative anatomy of marmoset and mouse cortex from genomic expression. J. Neurosci. 32, 5039–5053. https://doi.org/10.1523/JNEUROSCI.4788-11.2012.

Muñoz, A., Méndez, P., DeFelipe, J., Alvarez-Leefmans, F.J., 2007. Cation-chloride cotransporters and GABA-ergic innervation in the human epileptic hippocampus. Epilepsia 48 (4), 663–673. https://doi.org/10.1111/j.1528-1167.2007.00986.x. doi:EPI986 [pii].

Paxinos, G., Franklin, K., 2001. The Mouse Brain in Stereotaxic Coordinates. Academic Press, San Diego.

Seress, L., Gulyas, A.I., Freund, T.F., 1992. Pyramidal neurons are immunoreactive for calbindin D28k in the CA1 subfield of the human hippocampus. Neurosci. Lett. 138, 257–260.

Seress, L., Gulyas, A.I., Ferrer, I., Tunon, T., Soriano, E., Freund, T.F., 1993. Distribution, morphological features, and synaptic connections of parvalbumin- and calbindin D28k-immunoreactive neurons in the human hippocampal formation. J. Comp. Neurol. 337 (2), 208–230. https://doi.org/10.1002/cne.903370204.

Slomianka, L., Drenth, T., Cavegn, N., Menges, D., Lazic, S.E., Phalanndwa, M., Chimimba, C.T., Amrein, I., 2013. The hippocampus of the eastern rock sengi: cytoarchitecture, markers of neuronal function, principal cell numbers, and adult neurogenesis. Front. Neuroanat. 7, 34. https://doi.org/10.3389/fnana.2013.00034.

Sloviter, R.S., Sollas, A.L., Barbaro, N.M., Laxer, K.D., 1991. Calcium-binding protein (calbindin-D28K) and parvalbumin immunocytochemistry in the normal and epileptic human hippocampus. J. Comp. Neurol. 308 (3), 381–396. https://doi.org/10.1002/cne.903080306.

Soltesz, I., Losonczy, A., 2018. CA1 pyramidal cell diversity enabling parallel information processing in the hippocampus. Nat. Neurosci. 21 (4), 484–493. https://doi.org/10.1038/s41593-018-0118-010.1038/s41593-018-0118-0. [pii].

Tapia-González, S., Insausti, R., DeFelipe, J., 2019. Differential expression of secretagogin immunostaining in the hippocampal formation and the entorhinal and perirhinal cortices of humans, rats and mice. J. Comp. Neurol. https://doi.org/10.1002/cne.24773.

van Dijk, R.M., Huang, S.-H., Slomianka, L., Amrein, I., 2016. Taxonomic separation of hippocampal networks: principal cell populations and adult neurogenesis. Front. Neuroanat. 10, 22. https://doi.org/10.3389/fnana.2016.00022.

Wittner, L., Eross, L., Szabo, Z., Toth, S., Czirjak, S., Halasz, P., Freund, T.F., Magloczky, Z.S., 2002. Synaptic reorganization of calbindin-positive neurons in the human hippocampal CA1 region in temporal lobe epilepsy. Neuroscience 115, 961–978.